Binuclear Pd(I)–Pd(I) Catalysis Assisted by Iodide Ligands for Selective Hydroformylation of Alkenes and Alkynes

Yang Zhang, Sebastian Torker, Michel Sigrist, Nikola Bregovic, Pawel Dydio

Binuclear Pd(I)–Pd(I) Catalysis Assisted by Iodide Ligands for Selective Hydroformylation of Alkenes and Alkynes

Yang Zhang[1], Sebastian Torker[1,2]*, Michel Sigrist[1], Nikola Bregović[1], and Paweł Dydio[1]*

[1] University of Strasbourg, CNRS, ISIS UMR 7006, 8 allée Gaspard Monge, 67000 Strasbourg, France

[2] Department of Chemistry, Merkert Chemistry Center, Boston College, Chestnut Hill, MA 02467, USA

ABSTRACT: **Since its discovery in 1938, hydroformylation has been thoroughly investigated and broadly applied in industry (>10^7 metric ton yearly). However, the ability to precisely control its regioselectivity with well-established Rh- or Co-catalysts has thus far proven elusive, thereby limiting access to many synthetically valuable aldehydes. Pd-catalysts represent an appealing alternative, yet their use remains sparse due to undesired side-processes. Here, we report a highly selective and exceptionally active catalyst system that is driven by a novel activation strategy and features a unique Pd(I)–Pd(I) mechanism, involving an iodide-assisted binuclear step to release the product. This method enables β–selective hydroformylation of a large range of alkenes and alkynes, including sensitive starting materials. Its utility is demonstrated in the synthesis of anti-obesity drug Rimonabant and anti-HIV agent PNU-32945. In a broader context, the new mechanistic understanding enables the development of other carbonylation reactions of high importance to chemical industry.**

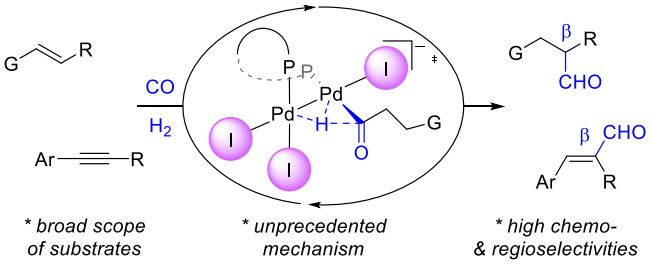

INTRODUCTION

Hydroformylation of alkenes and alkynes is the method of choice for the synthesis of versatile aldehydes.[1–4] Since the reactions typically yield mixtures of regioisomeric products, fine-chemical synthesis requires the ability to control precisely the regioselectivity of these processes, founding a compelling but often unaddressed problem.[5–7] Because of inherent selectivity preferences, Pd-based catalysts[8–11] could complement well-established Rh-based catalysts for reactions with alkenes such as vinyl arenes, enamides or acrylates (Figure 1a).[12–18] However, the utility of these protocols is limited due to requirement of a strong Brønsted acid co-catalyst and high temperatures (e.g., *p*-toluenesulfonic acid at 100-125 °C). Such conditions are not suitable for numerous substrates, including oligomerization-prone (electron-rich) vinyl arenes, or substrates containing acid-sensitive functional groups (e.g., acetal, silyl, N-Boc). Furthermore, the formation of aldehydes is typically accompanied by undesired formation of ketones, CO/alkene copolymerization, and hydrogenation processes.[8,9]

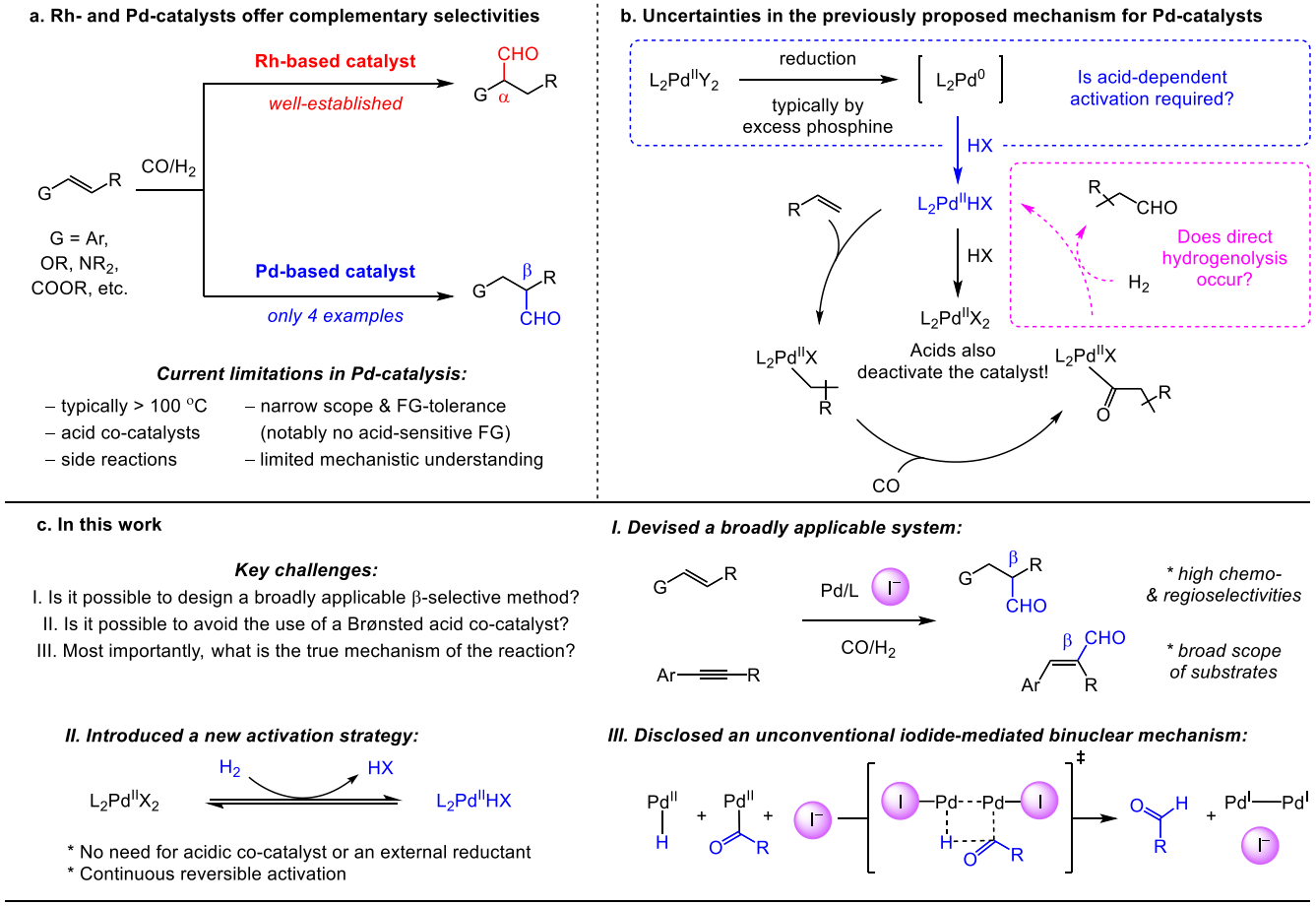

Figure 1. Hydroformylation of functionalized alkenes. (a) State of the art for Rh- and Pd-catalysis. (b) Plausible mechanism of Pd-catalyzed reactions. (c) Summary of this work.

Because of limited experimental and theoretical insight,[19] the mechanistic proposals for Pd-catalyzed hydroformylation remain to a large degree speculative, hampering further rational development of new protocols (Figure 1b). For instance, the empirically determined requirement for a Brønsted acid co-catalyst is typically attributed to pre-catalyst activation,[8–10] while excess phosphine ligand is applied as the reductant for catalyst activation. In contrast, related Pd-catalyzed carbonylation reactions were reported to occur in the absence of a Brønsted acid,[20] and a number of other pathways to generate the catalytically active species have been suggested.[21] Common to all proposed catalytic cycles is the involvement of Pd-acyl species, observed as intermediates in several carbonylation reactions.[22] These Pd-acyl species are typically suggested to undergo hydrogenolysis with dihydrogen to release the aldehyde product.[8,9,23] Nonetheless, Beller and colleagues reported that such an elementary step might be challenging and requires specific ligands and basic additives.[24]

In order to address the reasons for low catalyst activity and the need for elevated reaction temperatures, we initiated our study with the following proposals:

(1) We speculated that the acidic conditions of previous hydroformylation protocols might not only limit the substrate scope, but also partially deactivate the catalytically active palladium hydrido complex ($L_2Pd(II)HX + HX \rightarrow L_2Pd(II)X_2 + H_2$; Figure 1b).[25]

(2) Additionally, we surmised that excess phosphine ligand, typically used as the reductant during catalyst activation, might inhibit certain elementary steps of the catalytic cycle[26] or favor the formation of off-cycle dormant complexes.[24,27]

(3) Therefore, we envisioned an alternative pathway for generation of the palladium hydrido species through heterolytic H_2 cleavage assisted by anions (Figure 1c),[25] a mechanism that would render the presence of a Brønsted acid and excess phosphine obsolete. We surmised that such a process would on one hand depend on the basicity of the anion, (thought to facilitate heterolytic H_2 cleavage), and on the other hand be influenced by the ability of the anion to coordinate to Pd, which could potentially block the active Pd site.

Herein we present, guided by the above design criteria, a broadly applicable iodide-dependent Pd-based protocol that enables β–selective hydroformylation of alkenes and alkynes, including starting materials that contain a range of (acid-sensitive) functional groups. Our mechanistic studies further reveal the origin for the high catalytic activity, which is attributed to both, the facile pre-catalyst activation with dihydrogen and an unconventional binuclear mechanism assisted by iodide ligands to release the product.

RESULTS AND DISCUSSION

Formulation of the catalyst.

Evaluation of effect of different anions. We commenced our studies by probing the activity of bisphosphine-Pd-complexes containing different anions in the absence of co-catalysts or protic solvents. We selected xantphos (4,5-bis(diphenylphosphino)-9,9-dimethyl-xanthene) as the model ligand, previously reported to form highly active Rh-based hydroformylation[28] and Pd-based carbonylation catalysts.[29,30] 1-Decene served as the initial robust model substrate (Figure 2a). No reaction (<2%) was observed with complexes containing an acetate, a trifluoroacetate, an acetylacetonate, a triflate, or a tetrafluoroborate counterion. In contrast, in the presence of complexes bearing a chloride, a bromide, or an iodide, the aldehyde products were generated readily and with complete chemoselectivity (Figure 2a); none of the commonly generated side-products, such as (poly)ketones, alcohols, or alkanes were detected.[8] Reaction in the presence of iodide as counterion was most efficient, affording the aldehydes exclusively (>99%; 58% regioselectivity for *n*-aldehyde). It should be noted that the Shell laboratories have reported an increase in rate and selectivity of Pd-catalyzed hydroformylation-hydrogenation tandem reactions of simple *internal* C_8-C_{10} alkenes to *linear alcohols* under syngas upon addition of sodium halide salts, but that Brønsted acids and high temperatures were still required. The rate increased up to 6–7-fold (sodium iodide < bromide ~ chloride), whereas the regioselectivity for the linear product increased from 65% to 82% in the reverse order (sodium chloride < bromide < iodide).[9] A halide anion was speculated to bind a proton during heterolytic dissociation of H_2, leading to formation of a Pd-acyl-hydride species. No experimental or theoretical data were reported to support such a hypothesis. Similarly, Shi and coworkers reported the accelerating effect of tetrabutylammonium iodide in Pd-catalyzed hydroformylation of alkenes with formic acid (used instead of syngas).[11] In the latter case, the iodide anion was proposed to facilitate ligand exchange to form a Pd-acyl-formate complex, which would release CO_2 and the aldehyde product. Again, no data were reported to support such a claim.

Evaluation of phosphine ligands. Because the activity and chemoselectivity (i.e., selectivity for hydroformylation over other side-reactions), have been reported to be sensitive to basicity, bite- and cone-angle of a phosphine,[8,10] we tested several other mono- and bidentate ligands in presence of PdI_2. For all of them the model reaction occurred with full chemoselectivity toward the aldehyde (e.g., with PCy_3, PPh_3, MePhos, dppf, rac-BINAP, DPEphos as ligands; Table S3), although regioselectivity and yields varied. For instance, the reactions in the presence of dppf–PdI_2 or DPEphos–PdI_2 provided similar regioselectivity and yields as the reaction with xantphos–PdI_2 (95-99% yield, 54-58% n-regioselectivity), while regioselectivity was higher with rac-BINAP–PdI_2 (82%), albeit at lower alkene conversion (21%). Noteworthy, monodentate PPh_3 and PdI_2 formed an active catalyst that furnished the model aldehydes in 93% yield and 49% n-selectivity.

Optimization of reaction conditions. We then evaluated reactions of functionalized alkenes that are prone to undergo side reactions (e.g., (co-)polymerization, hydrogenation processes).[8] In the presence of 1 mol% xantphos–PdI_2 and syngas, styrene (**1a**) was consumed completely (>99% conv.), but there was only 11% of aldehyde **2a** formed with 76:24 β:α selectivity (Figure 2b). The remaining starting material was converted to a complex mixture of products as the result of oligomerization and hydrogenation side

reactions. Varying the reaction conditions (e.g., solvent, temperature, or pressure) did not lead to a significant improvement of the yield of **2a**.[31]

Next we turned to Lewis acid additives, which have been demonstrated by Dobereiner and Becica to accelerate amide N-aryl formation catalyzed by a xantphos–Pd complex.[32] The rate enhancement was proposed to originate from reversible ligand abstraction to create an open ligation site for substrate coordination. We indeed observed an increase in activity of xantphos–PdI_2 the presence of 0.2 mol % $Al(OTf)_3$ or $In(OTf)_3$ (Figure 2b). In sharp contrast, and in line with our mechanistic assumptions, the addition of 0.2 mol % $PPh_4^+I^-$ or excess xantphos (0.2 mol %) slowed down or completely inhibited the reaction. Furthermore, the addition of Brønsted acids lowered yields of aldehydes to < 10% and promoted hydrogenation processes (66% or 71% yield of ethylbenzene formed, in the presence of AcOH or TsOH, respectively).

To eliminate the need for the presence of a strong Lewis acid that may trigger side reactions, we tested whether excess PdI_2 (without dative ligands) could also serve to reversibly abstract ligands. Indeed, with 0.2 mol % PdI_2 instead of a Lewis acid, the reaction was also accelerated (Figure 2b). Similar enhancement was observed by the addition of $Pd(OAc)_2$ (the latter is soluble in organic solvents, alike xantphos–PdI_2, allowing for ease of manipulation in solution). In addition, 1 mol% xantphos–PdI_2 and 0.2 mol% $Pd(OAc)_2$ also allow for the transformations to be carried out efficiently at lower temperature. At 70 °C, **1a** was converted to the aldehydes in nearly quantitative yield, with 78% β selectivity. At 50 °C, the reaction was slower (65% conversion, using double the standard catalyst loading), but the aldehyde was formed with higher regioselectivity (85% β-aldehyde).

Evaluation of substrate scope of alkenes. The method proved to be broadly applicable (Figure 2c). Styrene derivatives containing an electron-withdrawing (**1b-1f**) or an electron-donating group (**1g-1j**), as well as those with a sizeable aromatic moiety (**1k**) were compatible substrates, generating the product with up to 90% β selectivity. Reactions with 1,1-disubstituted olefins (**1l-1n**) were similarly efficient and highly regioselective (93-99% β). A range of vinyl and allyl substrates **1q-1u** also underwent hydroformylation to form aldehydes with high β selectivities (90%-99%). Notably, acrylates **1v-1w**, which have been reported to co-polymerize with CO in the presence of Pd-based hydroformylation catalysts,[33] reacted smoothly (94-99% β selectivity and 81-99% yield). Remarkable are also transformations involving acid-sensitive N-Boc-N-vinylformamide **1u** and acetal **1x**, which are incompatible with the acidic conditions of previous Pd-based hydroformylation protocols, are compatible with the new method (81-94% β selectivity and 33-81% yields). Linear and cyclic aliphatic alkenes (**1y-1z**) were compatible as well; albeit the reactions required higher temperature (100 °C). Notably, alkene substrates containing unprotected N-H or O-H bonds or strongly coordinating groups, such as pyridyl moiety, failed to deliver the aldehyde product, illustrating current limitations of the method (Scheme S1).

Because 1,2-disubstituted aryl olefins, such as trans-isomethyleugenol **1o** or trans-β-methylstyrene **1p** are prone to undergo isomerization, especially at elevated temperatures, hydroformylation typically results in a mixture of aldehydes with either the α or γ isomer being the main product.[34] With the new conditions, however, **1o-1p** reacted to form β aldehydes predominantly (62-69% β selectivity; Figure 2d). Remarkably, β selectivity was partially maintained at higher temperatures, albeit hydrogenation diminished the yield of aldehydes. Interestingly, methyleugenol **1o'** and allylbenzene **1p'**, the terminal alkene analogues of **1o-1p**, reacted to form aldehyde products with similar regioselectivity, suggesting facile isomerization and an inherent (moderate) β-selectivity under these conditions. Likewise, hydroformylation reactions of monosubstituted **1aa** as well as *Z*-1,2-disubstituted aliphatic olefin **1ab** produce the same linear aldehyde product (Figure 2e).

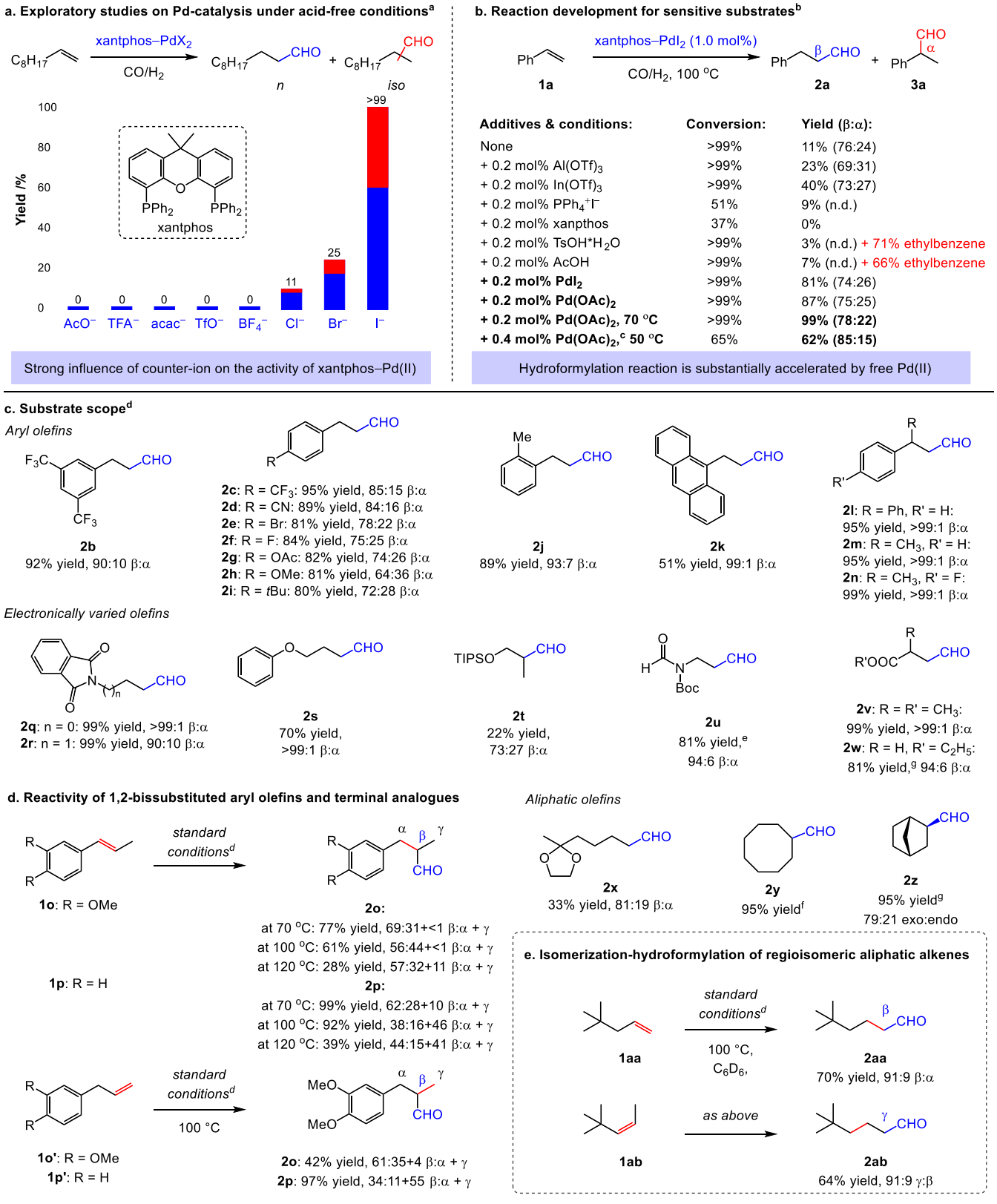

Figure 2. Hydroformylation of alkenes. [a] Reactions with 1 mmol 1-decene, 1.0 mol % PdX_2, 1.1 mol% xantphos, 20/80 bar of CO/H_2, 2 ml dioxane, 100 °C, 16 h. For the results of reactions in other solvents or with other ligands in place of xantphos, see Section 3 of the Supporting Information. [b] Reactions with 0.125 mM alkene in toluene. [c] 2.0 mol% xanpthos–PdI_2. [d] Reactions with 0.125 mM alkene, 1.0 mol% xanpthos–PdI_2, 0.2 mol% $Pd(OAc)_2$, 20/80 bar of CO/H_2, toluene, 70 °C, 16 h. [e] 5-fold catalyst loading. [f] 100 °C. [g] 0.5 mM alkene in 1,4-dioxane, CO/H_2 20/80 bar, 1 mol% PdI_2, 1.1 mol% xantphos, 100 °C. Conversion, yield, and regioselectivity determined by analyses of GC traces and ^1H NMR spectra with a standard (1,3,5-trimethoxybenzene or 1,4-dimethoxybenzene).

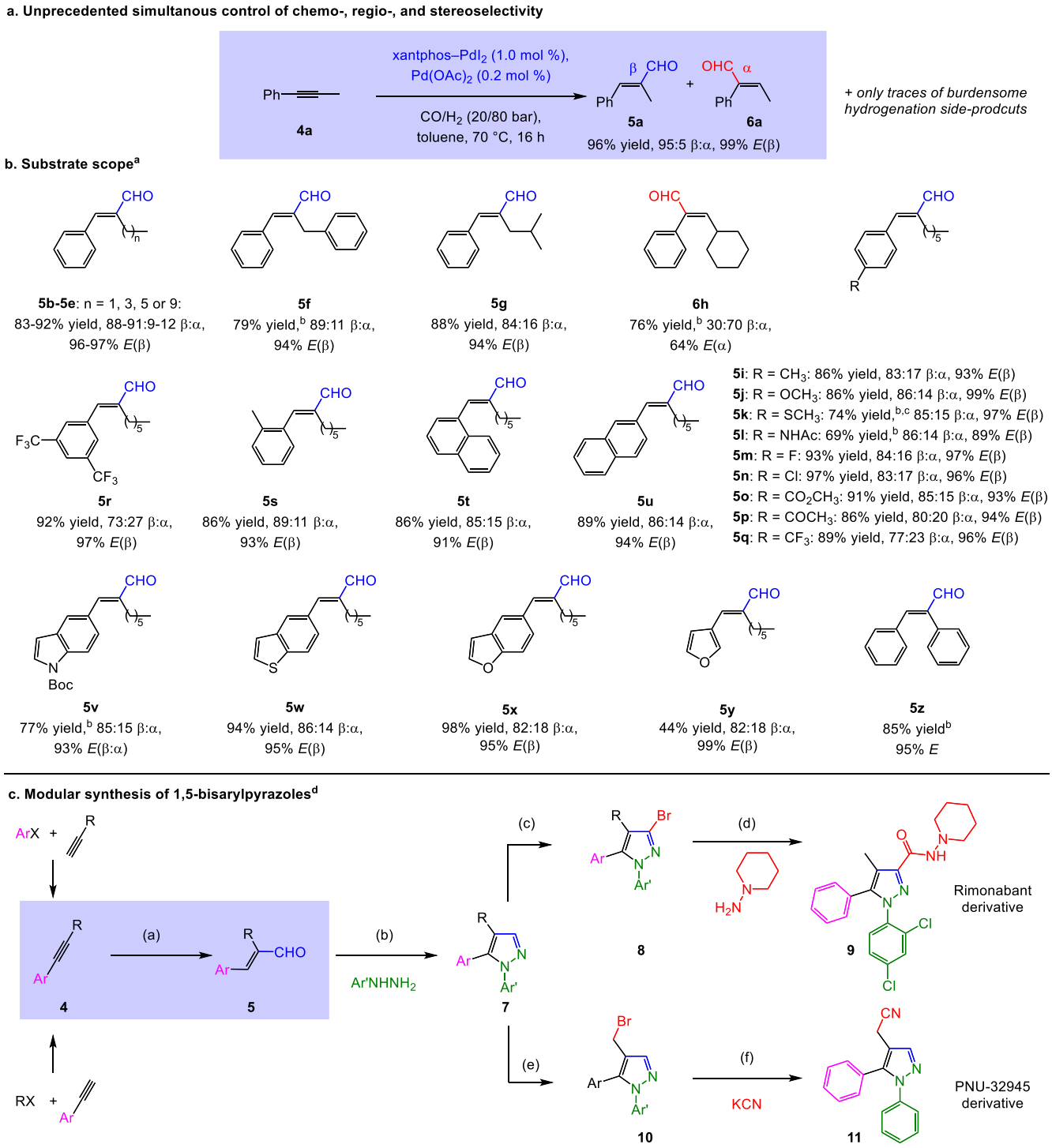

Figure 3. Hydroformylation of alkynes (a,b) & synthesis of bisarylpyrazoles (c). [a] Reactions with 0.125 mM alkyne. [b] 2.0% cat. [c] 82% conv. Yield and regioselectivity determined by analysis of ^{1}H NMR spectra with an internal standard (1,3,5-trimethoxybenzene or 1,4-dimethoxybenzene). [d] Conditions: (a) For 1.2 g of methylphenylacetylene (4a), PdI_2 (1.0 mol%), xantphos (1.0 mol%), $Pd(OAc)_2$ (0.2 mol%), CO/H_2 (20/80 bar), toluene, 70 °C, 18 h, 83% yield; (b) Ar'$NHNH_2$*HCl (1.5 equiv.), I_2 (1.5 equiv.), EtOH, reflux, 18 h; 74% yield for R = CH_3, Ar = Ph, Ar' = 2,4-Cl_2Ph; 41% yield for R = CH_3, Ar = Ar' = Ph; (c) NBS (1.1 equiv.), $AlCl_3$ (10 mol%), CH_3CN, 80 °C, 80% yield for R = CH_3, Ar = Ph, Ar' = 2,4-Cl_2Ph; (d) 1-aminopiperidine (1.5 equiv.), $Pd(OAc)_2$ (2 mol%), P(t-Bu)$_3$ (6 mol%), tetramethylethylenediamine (TMEDA, 0.75 equiv.), CO (40 bar), dioxane (0.125 M), 120 °C, 58% yield; (e) NBS (1.1 equiv.), azobisisobutyronitrile (AIBN, 5 mol%), CCl_4, reflux, overnight; (f) KCN (1.1 equiv.), DMSO, 22 °C, 30 min, 45% yield (over 2 steps).

Hydroformylation of alkynes. Next, we turned our attention to alkynes. The hydroformylation of alkynes constitutes an appealing strategy to produce enals, which are valuable building blocks in synthesis and occur as structural motives in natural or synthetic products (e.g., fragrances or flavors). However, despite many efforts, the hydroformylation protocols for their generation remain largely undeveloped.[35–40] Besides controlling regioselectivity, a key challenge is to prevent undesired side reactions, which mainly include hydrogenation of both starting materials and products. Previous efforts have shown that the chemoselectivity of the reaction can be adjusted by carefully designed catalysts and optimized reaction conditions;[35–39] however, control over regioselectivity remains largely unsolved. For instance, under state-of-the-art Rh-based[35] or Pd-based[36] protocols, methylphenylacetylene (**4a**) reacted to form a mixture of regioisomeric aldehydes **5a**:**6a** in 62:38 ratio, 78% combined yield along with 10% hydrogenation products, or in 21:79 ratio, 70% combined yield at 100% conversion of starting material, respectively (Figure 3a).

We found that in the presence of xantphos–PdI_2 and $Pd(OAc)_2$, the reaction of **4a** furnished enals with an unprecedented selectivity of **5a**:**6a** 95:5, 99:1 *E*:*Z* (**5a**), and 96% yield (Figure 3a). Control experiments confirmed that the presence of an iodide as well as the use of $Pd(OAc)_2$ as a co-catalyst are critical for activity and chemoselectivity. No reaction occurred when xantphos–PdI_2 was substituted by an analogue containing a different anion, or when $Pd(OAc)_2$ (or PdI_2) was absent.[31] Furthermore, the iodide also appears to be instrumental in controlling regioselectivity. This feature is highlighted by the control reaction in presence of xantphos–$Pd(acac)_2$ and *p*-TsOH, which only led to formation of enals in low regioselectivity and yield (**5a**:**6a** 68:32, 14% yield). These results suggest an active role of the iodide in the product-forming step.

Evaluation of substrate scope of alkynes. The catalytic protocol can be applied to a broad range of alkynes to form β-aryl enals, which were inaccessible through previous hydroformylation protocols (Figure 3b). Reactions with alkynes **4b**-**4e**, containing longer aliphatic moieties than **4a**, produced the aldehydes with high β regioselectivities (88-91%) and yields (83-92%). Derivatives bearing larger benzyl (**4f**) or iso-butyl (**4g**) groups also reacted with high β regioselectivities (89% and 84%) and yields (79% and 88%, respectively). In contrast to the former examples, an alkyne containing a sterically demanding cyclohexyl (**4h**) group reacted to form α-aldehyde **6h** as the major isomer (70%). Alkyne derivatives with an electron-donating or an electron-withdrawing group in the para-, meta-, or ortho-position of the phenyl ring (**4i**-**4s**), as well as those with a sizeable aryl moiety (**4t**-**4u**) were effective substrates, furnishing the product with up to 90% selectivity for β isomer. Particularly noteworthy are the transformations involving heteroaryl alkynes, bearing sensitive N-Boc-indole (**4v**), benzothiophene (**4w**), or (benzo)furan (**4x**-**4y**), which delivered β aldehydes in 82-86% regioselectivity and yields up to 98%. Selectivity issues aside, starting materials containing these sensitive moieties have previously not been reported to be compatible with Pd-based hydroformylation protocols. Notably, similar to the scope of alkenes, alkyne substrates bearing unprotected N-H, a strongly coordinating pyridine ring, or a terminal alkyne bond were not compatible, defining the limitations of the method (Chart S1).

Synthesis of bisarylpyrazoles

With an efficient β-selective hydroformylation method for alkynes in hand, we devised a 4-step modular synthesis of 1,5-bisarylpyrazole derivatives (Figure 3c), which are at the core of many pharmaceuticals and agrochemicals.[41–44] The sequence starts with the hydroformylation of alkynes (either commercially available or easily accessible[45]) followed by I_2-mediated oxidative condensation of enal **5** with an arylhydrazine to assemble pyrazole derivative **7**.[46] The subsequent selective electrophilic bromination of the pyrazole ring in **7** with N-bromosuccinimide (NBS) to form **8** enables diversification of the 5-position. For instance, 5-bromopyrazole **8** reacted with 1-aminopiperidine under a CO atmosphere in the presence of a palladium complex to furnish **9**, a Rimonabant derivative, i.e., a cannabinoid-1 receptor antagonist previously used as an appetite suppressant.[47] Alternatively, in the presence of a radical initiator (azobisisobutyronitrile, AIBN), **7** reacted with NBS at its alkyl site to form 4-(bromomethyl) derivative **10**, which was reacted directly (in one-pot) with KCN[48] to form **11**, PNU-32945, a HIV-1 reverse transcriptase inhibitor.[49] The above examples showcase that, starting from simple commercial building blocks, numerous derivatives of such biologically active molecules can be rapidly accessed.

Mechanistic studies

Having demonstrated utility of the method, open questions remained regarding the mechanistic aspects of this reaction. In particular we wondered whether activation of the pre-catalyst occurred as hypothesized (see above) and whether the activation process would determine the overall activity of the catalyst or whether other factors would be rate-limiting. Equally unclear was the unique role the halide anions played in the reaction and why the addition of free $Pd(OAc)_2$ (or PdI_2) had an accelerating effect. When and how the regioselectivity was established remained to be solved as well. To shed light onto the above questions, we performed detailed experimental studies, which we further corroborated with DFT calculations.

Activation of the palladium-complex (generation of Pd-hydride species). In agreement with our initial hypothesis, a series of xantphos–Pd(II) complexes bearing weakly coordinating anions readily formed Pd-hydride species under syngas without the need for any Brønsted acid co-catalyst (Figure 4a). In particular, the formation of fluxional cationic binuclear Pd(I)–Pd(I) hydridocarbonyl complex $[(xantphos)_2Pd_2(\mu\text{-}H)(\mu\text{-}CO)]^+$ (**Pd_2–hydride$^+$**) was indicated by the characteristic quintet hydride signal in the ^1H NMR spectrum as well as doublet and singlet signals in the proton-coupled and proton-decoupled ^{31}P NMR spectra, respectively.[19,50–55] The structure was further confirmed by x-ray analysis for **Pd_2–hydride$^+$** bearing a trifluoroacetate counterion. Additionally conducted isotope-labelling experiments with D_2 confirmed the source of the hydride atom; reaction of xantphos–Pd(II) trifluoroacetate and D_2/CO in CH_2Cl_2 furnished $[(xantphos)_2Pd_2(\mu\text{-}D)(\mu\text{-}CO)]^+$, **$Pd_2$–deuteride$^+$** complex, with a characteristic quintet deuteride signal in the ^2H NMR spectrum and a triplet signal in the proton-decoupled ^{31}P NMR spectrum (Figures S30-S31).[31] A plausible mechanism for formation of the binuclear Pd(I)–Pd(I) complexes, consistent with the observations of the activation reactions under dihydrogen (Figures S35-S36),[31] is depicted in Figure 4b. Notably, because formation of the Pd-hydride is accompanied by formation of a molecule of Brønsted acid that favors the reverse reaction,[25,52] the process remains reversible. It appears that the base is not required for the activation, but its presence (Et_3N) can profoundly impact the equilibrium of the various Pd species (most noticeable in case of HI generation). In the absence of a base xantphos–PdI_2 dominates the equilibrium, while in the presence of a stochiometric amount of base **Pd_2–hydride$^+$** or xantphos–PdHI are formed (under syngas or dihydrogen, respectively). Furthermore, an excess of base drives these reactions towards the Pd(0) species.[31] It should be pointed out that under catalytic conditions, the strong acid (e.g., HI) can be quenched by the alkene (e.g., hydrohalogenation of alkene **1q**, Figure S65). We also found that the formation of **Pd_2–hydride$^+$** is fully inhibited for the complexes bearing an acetate or an acetylacetonate (anions of typical catalyst precursors).[8,10,36] Notably, Poli, Drent and coworkers reported the formation of a mixture of a related binuclear Pd(I)–Pd(I) carbonyl hydride complex and a binuclear Pd(I)–Pd(I) biscarbonyl complex in the reaction of preformed BCOPE–$Pd(OTf)_2$ with syngas (BCOPE = (c-C_8H_{14}-1,5)PCH_2CH_2P(c-C_8H_{14}-1,5)).[19] Although, a mixture of $Pd(OAc)_2$, excess BCOPE, and TfOH and water was catalytically active in hydroformylation-hydrogenation tandem reactions,[9] neither the catalytic competency of binuclear Pd(I)–Pd(I) species bearing BCOPE nor their formation under the actual catalytic conditions were reported.[19]

Reaction intermediates (Pd-acyl vs Pd-alkyl). Our initial focus was directed towards the structure and stability of prospective Pd-acyl intermediates, both in solution and in the solid state. Reaction of a xantphos–Pd(II) complex bearing a weakly coordinating anion, alkene **1q**, and syngas leads to formation of the cationic Pd-β-acyl species, **Pd-β-acyl$^+$** (Figure 4c). **1q** was chosen as a substrate due to its easy to monitor NMR signatures. The same cationic Pd-β-acyl species was formed in direct reactions of **1q** with isolated **Pd_2–hydride$^+$** in the presence or absence of iodide anions (under inert conditions). The structure of **Pd-β-acyl$^+$** was confirmed through x-ray analysis of the tetrafluoroborate complex, wherein the fourth site of the square-planar complex is occupied by the oxygen of trans-chelating xantphos. Analysis of the Pd-acyl species in solution at room temperature (NMR) reveals no dependence on the identity of the anion.[31] At temperatures below –20 °C, however, the NMR signals change significantly for the iodide complex, suggesting the existence of a pronounced degree of Pd-I interaction. Furthermore, control experiments for analogues of Pd-alkyl species bearing different anions (**Pd–alkyl$_{Me}^+$**), that is, the prospective intermediates connecting the Pd-hydride and the

Pd-acyl species, confirmed that CO insertion into the Pd-alkyl bond is rapid in all cases (Figure 4d).[31,56] The latter results are consistent with non-detectable amounts of Pd-alkyl species during the NMR studies under syngas.

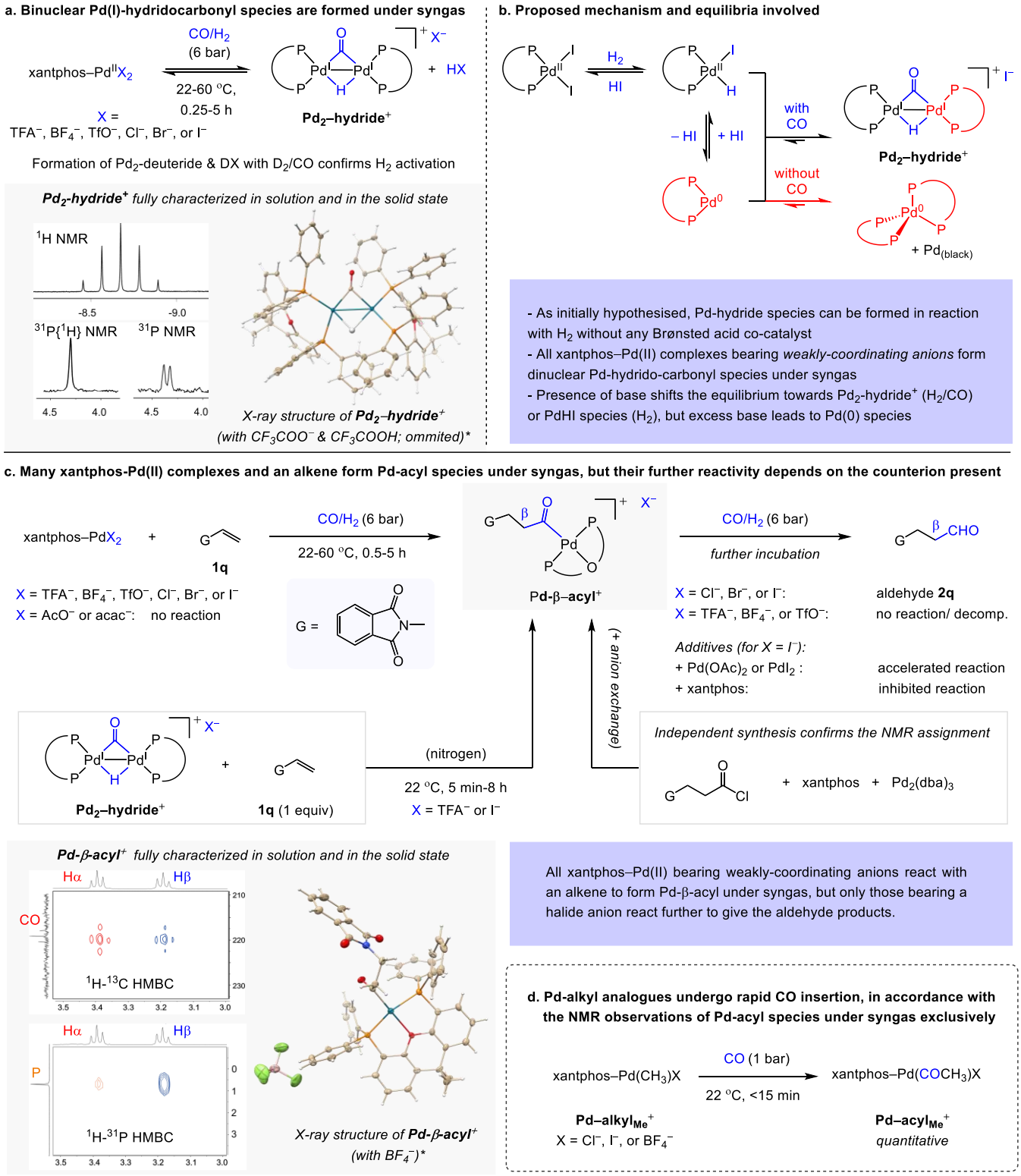

Figure 4. Investigation of reactivity of xantphos–Pd(II) complexes under syngas – influence of anions and additives. Reactions were performed in CD_2Cl_2 6 bar H_2/CO (or 1 bar CO) using 2 equiv. alkene **1q**; the progress was monitored by the NMR spectroscopy. * The hydride atom was located from the Fourier difference map and then refined with the AFIX1 constraint; anions in both structures are disordered; one position of BF_4^- is shown for clarity; thermal ellipsoids are drawn at 20% level; for ORTEP presentations at 50% level and further details, see the SI.

Release of the aldehyde product. Although the treatment of **1q** and a series of xantphos–Pd(II) complexes under syngas leads to formation of **Pd-β-acyl**$^+$, release of the aldehyde product **2q** occurs only in presence of halides, most readily iodide (Figure 4c). This step, which appears to be the bottleneck of the reaction, is further inhibited by excess xantphos or accelerated by catalytic $Pd(OAc)_2$ or PdI_2 additives.[31]

A series of stochiometric experiments with independently prepared **Pd-β-acyl**$^+$ complexes indicated that, in contrast to former proposals,[23] **Pd-β-acyl**$^+$ does not react directly with dihydrogen (Figure 5a).[31] Notably, the presence of iodide anions did not promote the reaction with dihydrogen, which is in contrast with the previous hypothesis on the role of halide anions by Leñero, Drent, and colleagues.[9] Moreover, **Pd-β-acyl**$^+$ did not undergo protonolysis with the Brønsted acids (HI, HCl, or TsOH), a process that would represent an alternative pathway to the formation of aldehydes.

Further experiments demonstrated that formation of the aldehyde occurs through a process involving Pd-hydride species and iodide anions (Figure 5a). Specifically, **Pd-β-acyl**$^+$ reacted readily with **Pd_2–hydride**$^+$ at room temperature in the presence of iodide forming aldehyde **2q** in 83% yield. No aldehyde was formed in the absence of iodide. This process was also accelerated by catalytic amounts of $Pd(OAc)_2$, but the presence of iodide ions was critical for the reaction to occur. These studies provide a clear evidence for the critical role of iodide, which is not to promote dihydrogen activation,[9] but to promote the reaction of **Pd-β-acyl**$^+$ with **Pd_2–hydride**$^+$.

Resting state and selectivity-determining step (stochiometric experiments). Although the pathways toward α– and β–aldehydes bifurcate already at the insertion of the alkene into the Pd–H bond, we established that this step does not control the regioselectivity of the reaction (as it does for a majority of Rh-catalyzed hydroformylation reactions).[1] Because the alkene and CO insertion steps are reversible, the regioselectivity is determined during conversion of Pd-acyls to aldehydes. The following two experiments were conducted to support such a scenario. (a) Reaction of **Pd-β-acyl**$^+$ (derived from alkene **1q**) in the presence of alkene **$1q_B$** led to the formation of a new Pd-β-acyl species (**Pd-β-$acyl_B^+$** bearing incorporated **$1q_B$**) and the free alkene **1q** (Figure 5b). (b) Alternatively, the independently prepared **Pd-α-acyl**$^+$ species was first converted into **Pd-β-acyl**$^+$ in presence of **Pd_2–hydride**$^+$ and iodide before it reacted to form β-aldehyde **2q** in 84% yield; again, no α-aldehyde **3q** was generated (Figure 5c). These results suggest that (i) not only does formation of both Pd-acyl species occur reversibly but that (ii) **Pd-β-acyl**$^+$ is thermodynamically more stable and, (iii) most importantly, also more reactive than **Pd-α-acyl**$^+$ during reaction with **Pd_2-hydride**$^+$ and iodide. The catalytic experiments with substrates containing electronically altered aryl groups with similar steric contribution (cf. Figure 2) further provide deeper insight into the relevance of electronic effects. It appears that the β selectivity in **2a-2i** as well as **2o-2o'** and **2p-2p'** correlate roughly with thermodynamic stabilities of the corresponding α and β aldehydes (i.e., electron-donating groups stabilize the electron-withdrawing formyl group),[57] consistent with a regioselectivity-determining transition state of the step in which the product is released. In short, it is therefore likely that both, higher thermodynamic stability, and higher reactivity of **Pd-β-acyl**$^+$ originate from a combination of steric and electronic effects. First, because of diminished steric requirements of the β-acyl ligand, with the steric bulk in **Pd-β-acyl**$^+$ being further away from the Pd site vs in **Pd-α-acyl**$^+$, and second, because the key transition state partly has the character of the product, electronic effects favor the thermodynamically more favored aldehyde product.

Identification of binuclear Pd complexes. Based on the stochiometric experiments between **Pd-β-acyl**$^+$ and **Pd_2–hydride**$^+$, we hypothesized that the prospective product-forming step could be a halide-mediated binuclear elimination reaction[58] between a Pd(II)-acyl species and a mononuclear Pd(II)-hydrido species; a step so far not considered for Pd-catalyzed hydroformylation.[23] The process would lead to the formation of a binuclear Pd(I)–Pd(I) complex (Figure 5d, insert). Initial support for such a mechanism was obtained through high-resolution mass-spectrometry of a reaction mixture between xantphos–PdI_2 and **1q** under syngas, which revealed a series of binuclear Pd(I)–Pd(I) complexes. Signals corresponding to [xantphos–Pd_2I]$^+$, [$(xantphos)_2$–Pd_2I]$^+$, and [$(xantphos)_2$–$Pd_2I(CO)$]$^+$ along with signals of other intermediates, i.e., mononuclear **Pd–hydride**$^+$ ([xantphos–PdH]$^+$), **Pd–alkyl**$^+$,

and **Pd–acyl$^+$** were observed (Figure 5d). Further, reaction of an independently prepared binuclear Pd(I)–Pd(I) complex, [(xantphos)$_2$–Pd$_2$](BF$_4$)$_2$, with syngas led to facile formation of the abovementioned catalytically active binuclear **Pd$_2$–hydride$^+$** complex (Figure 5e), in accordance with the involvement of binuclear Pd(I)–Pd(I) complexes in the catalytic cycle. Most interestingly, binuclear complex [(xantphos)$_2$–Pd$_2$](BF$_4$)$_2$ reacts with syngas to form **Pd$_2$–hydride$^+$** much faster than mononuclear complex xantphos–Pd(BF$_4$)$_2$ does (< 10 min at 22 °C vs. > 2 h at 60 °C).

X-ray analyses of several binuclear xantphos-Pd(I)–Pd(I) complexes gave insight into their structural features. While, in **Pd$_2$–hydride$^+$**, each xantphos is bound to the same Pd-center (in a *cis* fashion), each ligand is coordinated to both Pd-centers (in a bridging fashion) in cationic complex [(xantphos)$_2$–Pd$_2$(NCCH$_3$)$_2$]$^{2+}$ and in neutral complex xantphos–Pd$_2$I$_2$ (Figure 5e). In the latter case, 4 binuclear units are arranged in a tetrameric macrocycle, stabilized by bridging iodide anions. Noteworthy, the square planar geometries of the neighboring Pd centers are perpendicular to each other (vide infra).

Kinetic studies and rate-determining step (catalytic experiments). To provide insight into the mechanism under actual catalytic conditions, we conducted detailed kinetic studies. First, by using a 5:1 mixture of xanptphos–PdI$_2$ to Pd(OAc)$_2$ to maintain the ratio of xantphos-ligated and non-ligated Pd species, we determined a reaction order of 2.0 (±0.1) in Pd, which is in agreement with a binuclear rate-limiting step involving Pd-acyl and Pd-hydride species. Next, we established the reaction to be of negative order in alkene **1q** (−1.0 (±0.1)), which is in accordance with the alkene and the **Pd-β-acyl$^+$** resting state competing for the reaction with Pd-hydride species. Because the catalytic activity is sensitive to the Pd : xantphos ratio, we also studied the stoichiometry of the catalyst in the turnover-limiting step by the method of continuous variations of concentrations of PdI$_2$ and xantphos, often referred to as a Job analysis.[59] The highest activity was observed at ~0.67 molar fraction of PdI$_2$ (Figure S99), indicating a catalytic species (or a transition state) with a 2:1 Pd : xantphos ratio in the turnover-limiting step. Additionally, the experiments with varied amount of iodide at constant concentrations of Pd and xantphos (fixed 2:1 ratio) indicated the highest activity in the presence of 2-4 equivalents of the anion (vs. xantphos), while the activity was significantly reduced outside of that range (Figure S100). Together, the above data imply a ~2-4:2:1 iodide : Pd : xantphos molecularity in the turnover-limiting step.

Resting state under catalytic conditions. To get insight into the reaction intermediates under catalytic conditions, we monitored the reaction progress *in situ* with the aid of high-pressure NMR spectroscopy. It was revealed that conversion of alkene **1q** was accompanied by the transient formation of one major intermediate, **Pd-β-acyl$^+$**, which is finally converted to the single product **2q** (Figure S101).[31] Analogous experiments with **Pd-α-acyl$^+$**, **Pd-β-acyl$^+$** or **Pd$_2$-β-hydride$^+$** and PPh$_4$I (iodide source) as catalysts in place of xantphos–PdI$_2$, painted a similar picture (Figure S102). Irrespective of the initial complex, conversion of **1q** to product **2q** was observed, along with the presence of the same **Pd-β-acyl$^+$** intermediate.[60]

Lastly, when the catalytic reaction using alkene **1q** and a mixture of deuterium and CO was monitored *in situ* with ^{2}H NMR spectroscopy, fast incorporation of deuterium into **1q**, at both α– and β– C-H sites of the vinyl bond, prior to formation of any observable amount of aldehyde **2q**, was observed (within <10 min; Figure 103).[31] These data indicate that the alkene insertion into the Pd-hydride bond occurs both quickly and reversibly to form both Pd-α-alkyl and Pd-β-alkyl species.

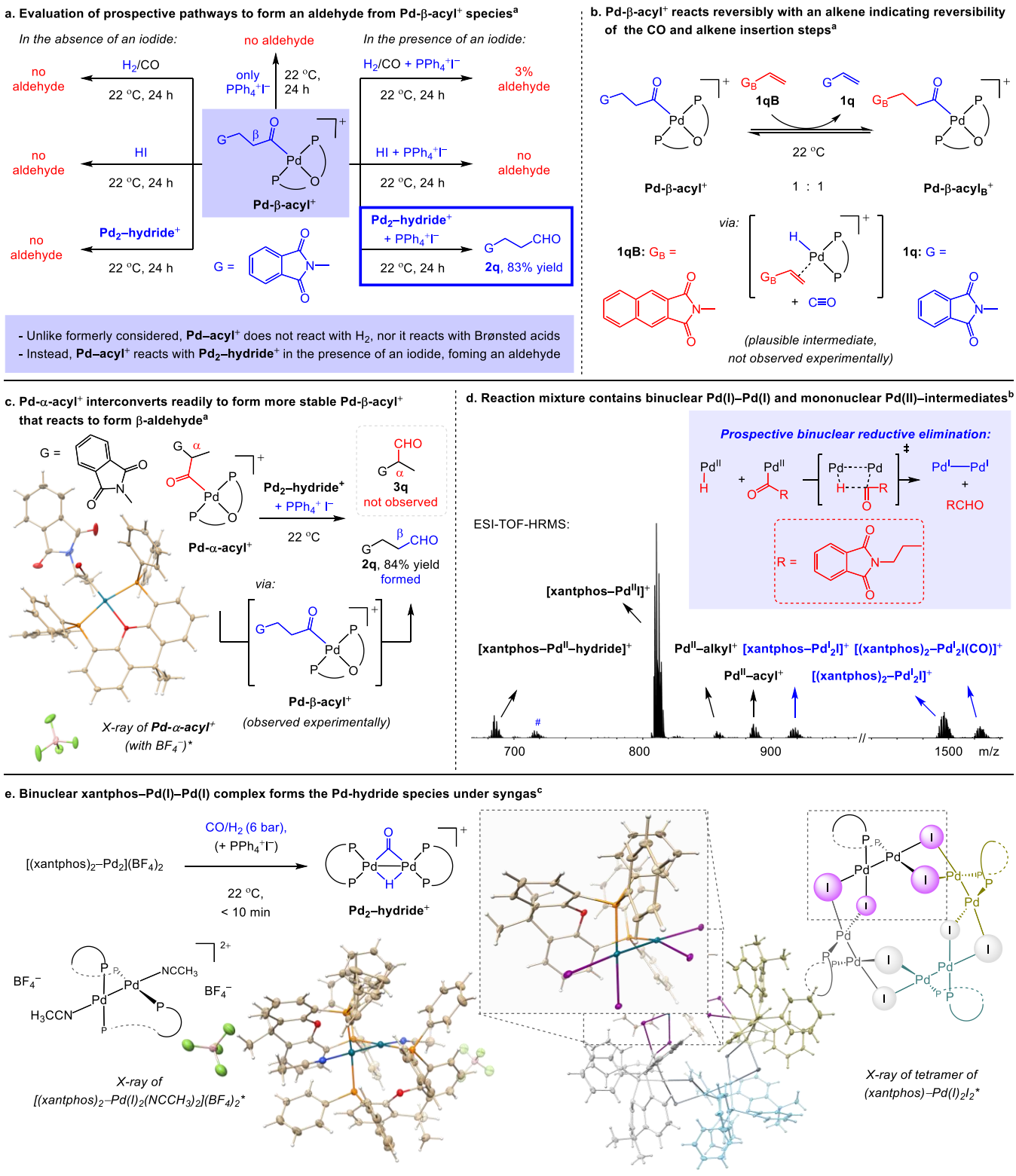

Figure 5. Investigation of reactivity of Pd(II)-acyl intermediates and binuclear Pd(I)-Pd(I) species. [a] Reactions were performed in CD_2Cl_2 under N_2 (or 6 bar H_2/CO) using 1 equiv. Pd-acyl bearing a tetrafluoroborate; 1 equiv. Pd-hydride bearing a trifluoroacetate; 1 equiv. $PPh_4^+I^-$ (per each Pd-complex); 1 equiv. HI; 1 equiv. **1qB**. The incubation of Pd-acyl species at higher temperatures led to decomposition. [b] Reaction mixture of xantphos-PdI_2 with alkene **1q** under syngas (6 bar) in CD_2Cl_2, at 50 °C for 6 h, was analyzed by ESI-TOF-HRMS; # – signals of [xantphos-Pd-H+O_2^+]. [c] Reactions in CD_2Cl_2. * Structure of Pd-acyl complex is disordered in the methyl group of the acyl ligand; structure of [(xantphos)$_2$-Pd(I)$_2$(NCCH$_3$)$_2$](BF$_4$)$_2$ is disordered in one phenyl group and one BF_4^-, disorder and co-crystalized CH_2Cl_2 are omitted for clarity; thermal ellipsoids are drawn at 20% level, except for the tetramer (50% level); for ORTEP presentations at 50% level, see the SI. For full experimental details, see the SI.

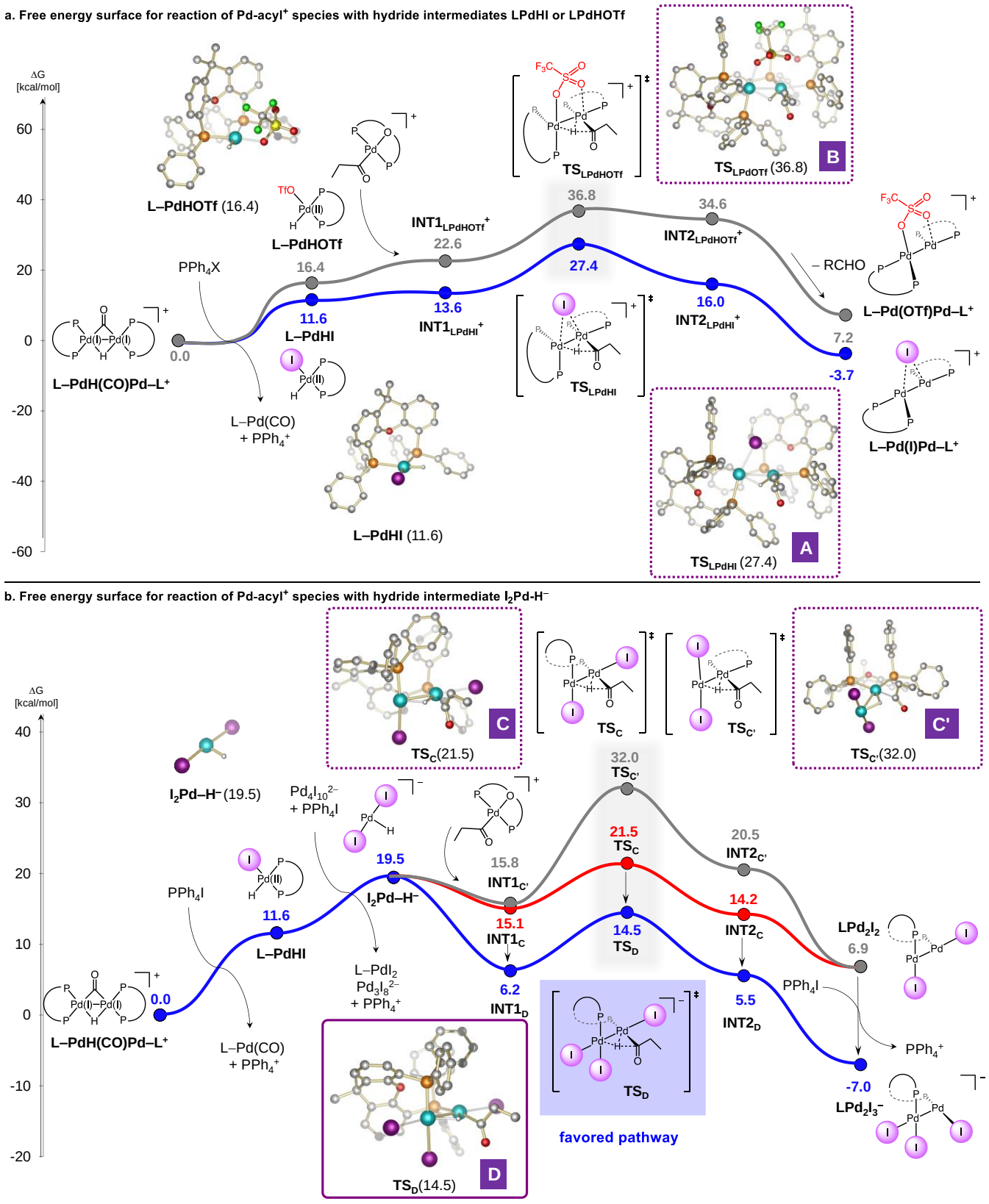

Figure 6. DFT investigation for binuclear reaction of Pd–acyl$^+$ with various Pd–hydride species. Calculations have been performed at the ωB97MV/def2-QZVPP//M06L/def2-SVP level of theory in dichloromethane as solvent (SMD solvation model); SMD, solvation model based on density; **INT1** and **INT2**, intermediates, **TS**, transition state. For full discussions, further details, and structures of all transition states and intermediates, see the SI.

Density Functional Theory (DFT) studies. The experimental findings were further corroborated by DFT calculations at the ωB97MV/def2-QZVPP//M06L/def2-SVP level of theory,[61,62] which indicate that a binuclear reductive elimination step is the most likely scenario for the reaction (Figure 6). Initial formation of a mononuclear xantphos−Pd-hydride species **LPdHX** (along with xantphos−Pd^0(CO))[63] from the binuclear **Pd_2–hydride$^+$** ground state is predicted to be less endergonic in the presence of iodide vs. a weakly coordinating triflate anion (ΔG_{rel} = +11.6 kcal/mol vs. +16.4 kcal/mol for **LPdHI** vs. **LPdHOTf**, respectively). In addition, reaction of these mononuclear Pd-hydride species with the **Pd–acyl$^+$** ground state via binuclear reductive elimination (transition states **A** and **B**) is significantly favored in presence of the stronger coordinating halide anion (ΔG_{rel} = +27.4 kcal/mol for X = iodide vs. +36.8 kcal/mol for X = triflate; Figure 6a). Since the presence of two xantphos ligands in transition states **A** and **B** might lead to significant steric crowding, we investigated the further activation of **LPdHI** by additional iodide anions and Pd(II) additives (modeled as $(PdI_2)_n$). While generating **I_2Pd–H$^-$** anion is even more endergonic (ΔG_{rel} = +19.5 kcal/mol, Figure 6b), its subsequent reaction with the **Pd–acyl$^+$** through transition state **C** is strongly favored most likely due to reduced steric crowding (ΔG_{rel} = +21.5 kcal/mol). The presence of an additional halide ion, as in anionic transition state **D**, leads to further stabilization of the coordinatively unsaturated complex **C** (ΔG_{rel} = +14.5 kcal/mol;), identifying the most favored scenario for the reaction.[31] It is important to stress out that the geometry of transition state **D** is in excellent agreement with the structure of xantphos−Pd_2I_2 determined through x-ray crystallography (Figure 5e), giving further credence to the computed reaction pathway. Moreover, these computational results are consistent with the facile reaction at room temperature observed during stochiometric experiments (Figure 5a). The stoichiometry of the binuclear transition state complex containing 3 iodide ligands and just one xantphos is further in line with the accelerating effect of free $Pd(OAc)_2$ (or PdI_2), the inhibition by excess xantphos ligand, and the stoichiometry determined by kinetic experiments (~2–4 iodide : 2 Pd : 1 xantphos). Whether the **I_2Pd–H$^-$** anion represents an actual intermediate or if one of the xantphos ligands is lost during the formation of the binuclear complex remains a subject of speculation. However, Hartwig and coworkers showed that related anionic "ligandless" arylpalladium halide species (Br_2PdAr^-) are catalytic relevant intermediates in presence of dative phosphines ligands in the Heck reaction,[64] and the catalytic role of other anionic palladium halide species has been recently elucidated in cross-coupling reactions.[65–67]

Additional calculations indicate that the energy barriers for aldehyde formation via direct hydrogenolysis of the **Pd–acyl$^+$** ground state by H_2 (transition state **E**; Figure 7a) or protonolysis by HI (transition state **F**; Figure 7b) are energetically more demanding (ΔG_{rel} = +27.1 and +22.6 kcal/mol, respectively). These findings are consistent with the lack of reactivity in the stochiometric experiments involving the Pd-acyl species and H_2 or HI at room temperature (Figure 5a).

It is worth mentioning that due to the presence of sizeable xantphos ligands, dispersion forces play a significant contribution to the relative energies of intermediates and transition states **A–F** (several tens of kcal/mol).[68] Given that the applied solvation model tends to rather overestimate intermolecular dispersion in solution,[69,70] easier generation of the monomeric hydride species from dimeric **Pd_2-hydride$^+$** is predicted when only partial nonlocal dispersion[61] is accounted for. Simultaneously, transition states **C** and **D** are further favored over **A**, **B**, **E** and **F** (for the discussion of a plausible origin, see section 8.4 of the SI and Figure S108).

Summarized mechanistic proposal. Based on the mechanistic data we propose that the halide-assisted Pd-catalyzed hydroformylation of alkenes occurs as shown in Figure 8. The key mechanistic features are:

(1) Activation of phosphine−Pd(II) complex with dihydrogen – step I – to form the Pd-hydride species is both, facile and reversible, with the binuclear hydrido-carbonyl complex, **Pd_2–hydride$^+$**, dominating the equilibrium under syngas. The formation of Pd-hydride species does not require the presence of a Brønsted acid as co-catalyst, in contrast to previous speculations.[8–10]

(2) Alkene insertion into the Pd-hydride bond – step II – to form cationic Pd-alkyl intermediates, **Pd–alkyl$^+$**, followed by CO insertion – step III – to form the cationic Pd-acyl species, **Pd–acyl$^+$**, are both fast and reversible.

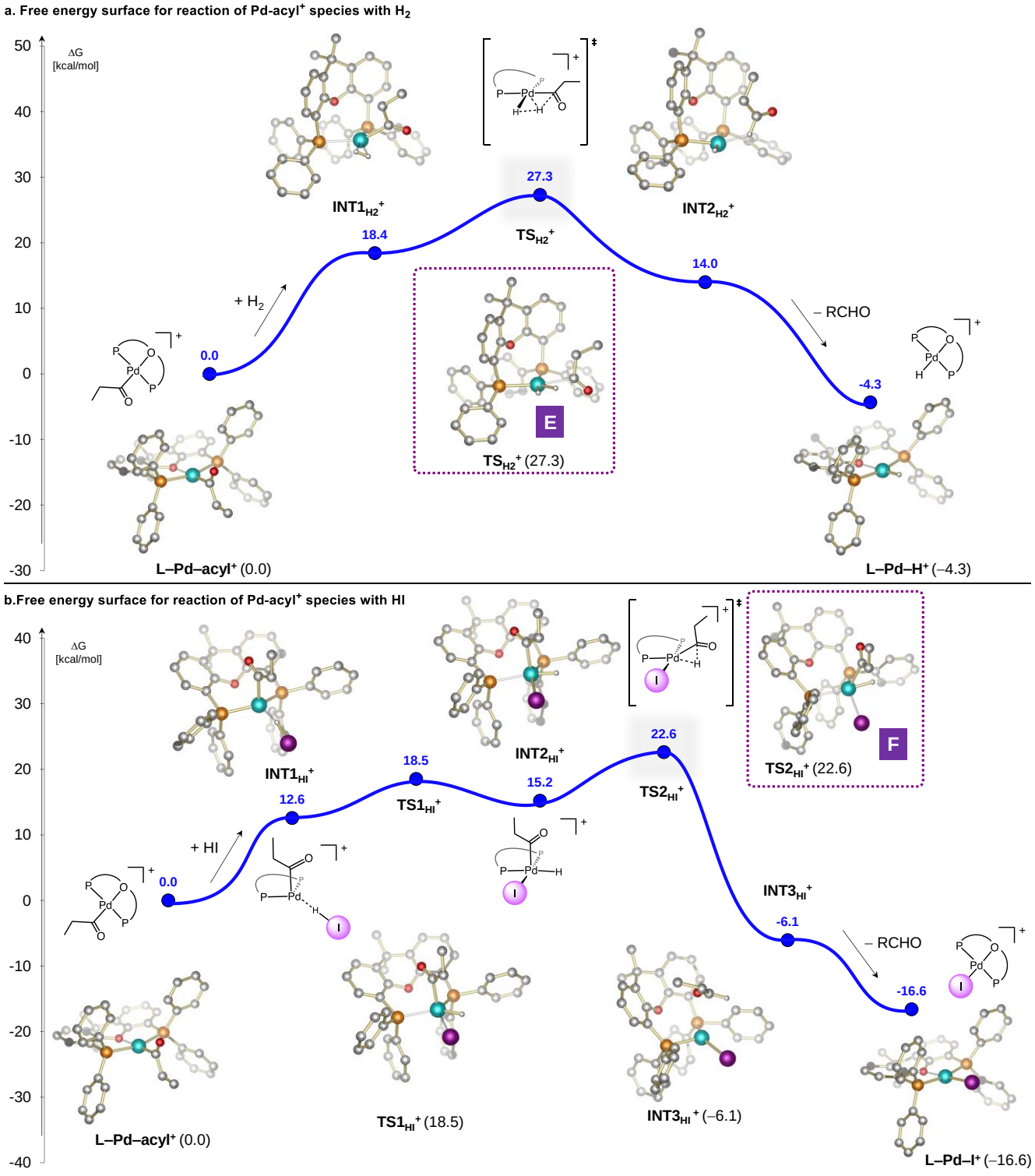

Figure 7. DFT investigation for mononuclear reaction of Pd–acyl$^+$ with H_2 or HI. Calculations have been performed at the ωB97MV/def2-QZVPP//M06L/def2-SVP level of theory in dichloromethane as solvent (SMD solvation model); SMD, solvation model based on density; **INT1**, **INT2**, and **INT3**, intermediates, **TS**, transition state. For full discussions, further details, and structures of all transition states and intermediates, see the SI.

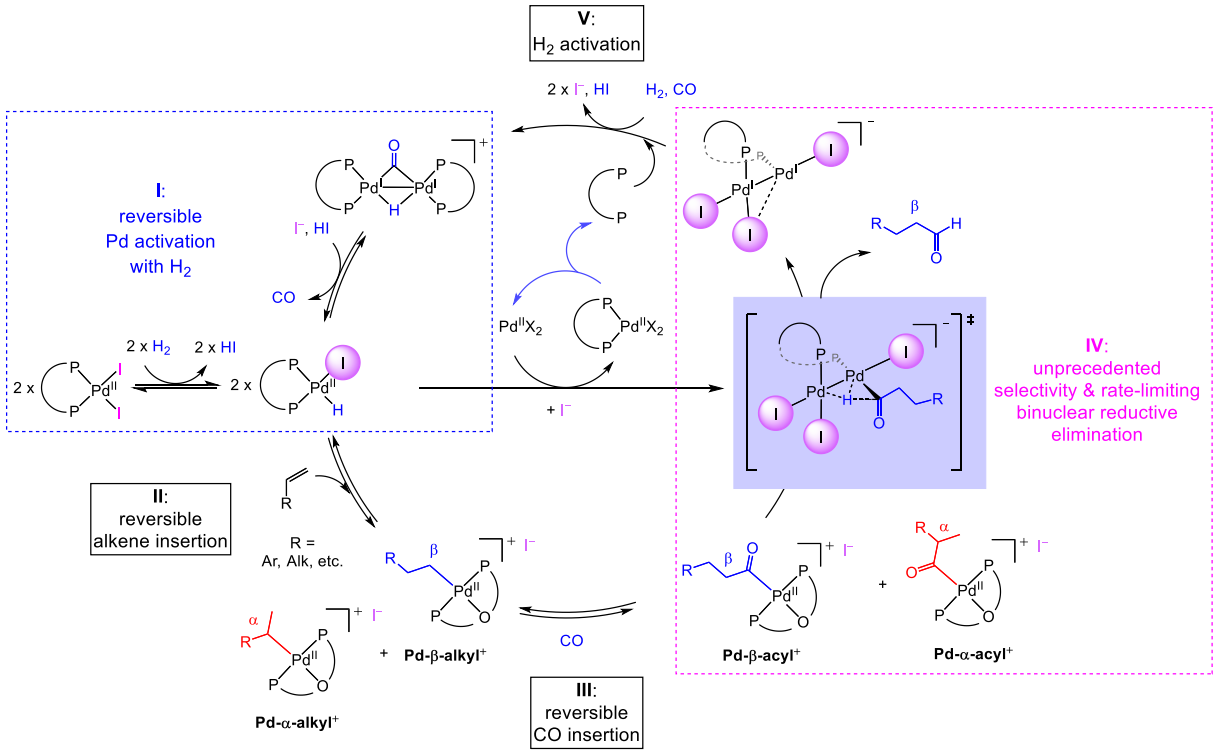

Figure 8. Full proposal of the mechanism of halide-assisted Pd-catalyzed hydroformylation of alkenes.

(3) **Pd–acyl$^+$** is the resting state of the catalytic cycle and does not react directly with dihydrogen, as had been proposed previously.[8,9,23] Instead, **Pd–acyl$^+$** reacts with a Pd-hydride species in the rate and selectivity determining step – step IV – via a binuclear elimination reaction[58] to form a Pd(I)–Pd(I) intermediate and the aldehyde product. The process is assisted by halides as ligands in accordance with the strong dependence of catalytic activity on the counterion. The proposed transition state geometry (3 iodide : 2 Pd : 1 xantphos) strongly correlates with the stoichiometry determined through kinetic experiments (2–4:2:1).

(4) In the final step the binuclear Pd(I)–Pd(I) intermediate reacts rapidly with H_2 under syngas – step V – to generate **Pd$_2$–hydride$^+$**, and HI. The acid then oxidizes this binuclear Pd(I)–Pd(I) hydrido species, furnishing two mononuclear Pd(II)-hydride species required for the catalytic turnover.

Noteworthy, binuclear cooperativity has been reported for some Co- and Rh-catalyzed hydroformylation processes;[13,58,71,72] however, a mechanistic proposal involving binuclear cooperativity in Pd-catalyzed hydroformylation as well as its dependence on the halide anions are unprecedented.

The herein proposed binuclear mechanism (Figure 6b) and the previously and more commonly invoked mononuclear process involving direct reaction of the Pd-acyl intermediate with H_2 (Figure 7a) are distinct from one another. Specifically, although the overall outcome is the same, the order of events appears to be altered. While it is an activated hydride species (a Pd(II)-hydride) that reacts with the Pd-acyl resting state in the binuclear mechanism (Figure 6b), heterolytic cleavage of H_2 across the Pd-acyl bond (as in Figure 7a) can be regarded as a protonation event of the acyl ligand (plus a hydride transfer to the Pd(II) cation). Why exactly such a reversal of events leads to a lowering of free energy is unclear at present, particularly given that direct comparison of transition states of significantly different nature is challenging. Further efforts directed towards deeper understanding of the herein proposed unique mechanism and evaluation of its validity in other Pd-catalyzed hydroformylation protocols with varied monodentate and bidentate ligands, as well as, its comparison to other more common metal catalyzed hydroformylation mechanisms (including Rh-based ones) are underway.

CONCLUSIONS

In conclusion, the herein disclosed hydroformylation strategy enables the production of a broad range of valuable aldehyde building blocks and products from feedstock materials and relies on an unconventional approach for activation of a palladium pre-catalyst. Additionally, our investigations elucidated a unique binuclear reaction mechanism and provide new insights regarding the positive influence of halide anions, a feature that had previously only been reported empirically in various palladium-catalyzed transformations.[9,11,73,74] Our preliminary data of high-yielding and highly selective alkoxy-, thio- and aminocarbonylation transformations (Figure S1) foreshadow extension of our methodology to lift existing limitations in other industrially important palladium-catalyzed carbonylation reactions used in the synthesis of highly valuable carbonyl compounds such as carboxylic acids, esters, thioesters, or amides.

AUTHOR INFORMATION

Corresponding Authors

* E-mails: dydio@unistra.fr; torker@unistra.fr

ACKNOWLEDGMENT

This work was financially supported by the University of Strasbourg, the French National Research Agency (ANR IdEx & ANR LabEx „Chemistry of Complex Systems“), The Frontier Research in Chemistry Foundation, and by the European Research Council (ERC StG „Reverse&Cat“ #804106). WCSS, http://wcss.pl, (No. 329) is acknowledged for resources in initial DFT studies. We are grateful to L. Karmazin and C. Bailly for solving and refining the x-ray crystal structures; K. Hurej for initial DFT studies and for assistance with some preliminary NMR experiments; and C. Antheaume and D. Lichosyt for assistance with some in situ NMR studies.

REFERENCES

(1) Leeuwen, P. W. N. M. van; Claver, C. *Rhodium Catalyzed Hydroformylation*; Kluwer Academic Publishers: New York, 2005.

(2) *Applied Homogeneous Catalysis with Organometallic Compounds: A Comprehensive Handbook in Three Volumes*; Cornils, B., Herrmann, W. A., Beller, M., Paciello, R., Eds.; Wiley-VCH Verlag GmbH & Co. KGaA: Weinheim, Germany, 2017. https://doi.org/10.1002/9783527651733.

(3) Franke, R.; Selent, D.; Börner, A. Applied Hydroformylation. *Chem. Rev.* **2012**, *112* (11), 5675–5732. https://doi.org/10.1021/cr3001803.

(4) *Hydroformylation: Fundamentals, Processes, and Applications in Organic Synthesis*; Börner, A., Franke, R., Eds.; Wiley-VCH Verlag GmbH & Co. KGaA: Weinheim, Germany, 2016. https://doi.org/10.1002/9783527677931.

(5) Cai, C.; Yu, S.; Cao, B.; Zhang, X. New Tetraphosphorus Ligands for Highly Linear Selective Hydroformylation of Allyl and Vinyl Derivatives. *Chem. - Eur. J.* **2012**, *18* (32), 9992–9998. https://doi.org/10.1002/chem.201201396.

(6) Yu, S.; Chie, Y.; Zhang, X. Highly Regioselective and Rapid Hydroformylation of Alkyl Acrylates Catalyzed by a Rhodium Complex with a Tetraphosphorus Ligand. *Adv. Synth. Catal.* **2009**, *351* (4), 537–540. https://doi.org/10.1002/adsc.200800676.

(7) Dydio, P.; Detz, R. J.; de Bruin, B.; Reek, J. N. H. Beyond Classical Reactivity Patterns: Hydroformylation of Vinyl and Allyl Arenes to Valuable β- and γ-Aldehyde Intermediates Using Supramolecular Catalysis. *J. Am. Chem. Soc.* **2014**, *136* (23), 8418–8429. https://doi.org/10.1021/ja503033q.

(8) Drent, E.; Budzelaar, P. H. M. The Oxo-Synthesis Catalyzed by Cationic Palladium Complexes, Selectivity Control by Neutral Ligand and Anion. *J. Organomet. Chem.* **2000**, *593–594*, 211–225. https://doi.org/10.1016/S0022-328X(99)00554-9.

(9) Konya, D.; Almeida Leñero, K. Q.; Drent, E. Highly Selective Halide Anion-Promoted Palladium-Catalyzed Hydroformylation of Internal Alkenes to Linear Alcohols. *Organometallics* **2006**, *25* (13), 3166–3174. https://doi.org/10.1021/om0601293.

(10) Jennerjahn, R.; Piras, I.; Jackstell, R.; Franke, R.; Wiese, K.-D.; Beller, M. Palladium-Catalyzed Isomerization and Hydroformylation of Olefins. *Chem. - Eur. J.* **2009**, *15* (26), 6383–6388. https://doi.org/10.1002/chem.200900700.

(11) Ren, W.; Chang, W.; Dai, J.; Shi, Y.; Li, J.; Shi, Y. An Effective Pd-Catalyzed Regioselective Hydroformylation of Olefins with Formic Acid. *J Am Chem Soc* **2016**, *138* (45), 14864–14867. https://doi.org/10.1021/jacs.6b10297.

(12) Leading studies on hydroformylation reaction with complexes of metals beyond rhodium: Hood, D. M.; Johnson, R. A.; Carpenter, A. E.; Younker, J. M.; Vinyard, D. J.; Stanley, G. G. Highly Active Cationic Cobalt(II) Hydroformylation Catalysts. *Science* **2020**, *367* (6477), 542–548. https://doi.org/10.1126/science.aaw7742.

(13) Hebrard, F.; Kalck, P. Cobalt-Catalyzed Hydroformylation of Alkenes: Generation and Recycling of the Carbonyl Species, and Catalytic Cycle. *Chem. Rev.* **2009**, *109* (9), 4272–4282. https://doi.org/10.1021/cr8002533.

(14) Wu, L.; Fleischer, I.; Jackstell, R.; Profir, I.; Franke, R.; Beller, M. Ruthenium-Catalyzed Hydroformylation/Reduction of Olefins to Alcohols: Extending the Scope to Internal Alkenes. *J. Am. Chem. Soc.* **2013**, *135* (38), 14306–14312. https://doi.org/10.1021/ja4060977.

(15) Kubis, C.; Baumann, W.; Barsch, E.; Selent, D.; Sawall, M.; Ludwig, R.; Neymeyr, K.; Hess, D.; Franke, R.; Börner, A. Investigation into the Equilibrium of Iridium Catalysts for the Hydroformylation of Olefins by Combining In Situ High-Pressure FTIR and NMR Spectroscopy. *ACS Catal.* **2014**, *4* (7), 2097–2108. https://doi.org/10.1021/cs500368z.

(16) Wu, L.; Liu, Q.; Spannenberg, A.; Jackstell, R.; Beller, M. Highly Regioselective Osmium-Catalyzed Hydroformylation. *Chem. Commun.* **2015**, *51* (15), 3080–3082. https://doi.org/10.1039/C4CC05626D.

(17) Pandey, S.; Raj, K. V.; Shinde, D. R.; Vanka, K.; Kashyap, V.; Kurungot, S.; Vinod, C. P.; Chikkali, S. H. Iron Catalyzed Hydroformylation of Alkenes under Mild Conditions: Evidence of an Fe(II) Catalyzed Process. *J. Am. Chem. Soc.* **2018**, *140* (12), 4430–4439. https://doi.org/10.1021/jacs.8b01286.

(18) A metal-free protocol of hydroformylation: Huang, H.; Yu, C.; Zhang, Y.; Zhang, Y.; Mariano, P. S.; Wang, W. Chemo- and Regioselective Organo-Photoredox Catalyzed Hydroformylation of Styrenes via a Radical Pathway. *J. Am. Chem. Soc.* **2017**, *139* (29), 9799–9802. https://doi.org/10.1021/jacs.7b05082.

(19) Baya, M.; Houghton, J.; Konya, D.; Champouret, Y.; Daran, J.-C.; Almeida Leñero, K. Q.; Schoon, L.; Mul, W. P.; Oort, A. B. van; Meijboom, N.; Drent, E.; Orpen, A. G.; Poli, R. Pd(I) Phosphine Carbonyl and Hydride Complexes Implicated in the Palladium-Catalyzed Oxo Process. *J. Am. Chem. Soc.* **2008**, *130* (32), 10612–10624. https://doi.org/10.1021/ja8012903.

(20) Scheele, J.; Timmerman, P.; Reinhoudt, D. N. A Significant Effect of Anion Binding Ureas on the Product Ratio in the Palladium(Ii)-Catalyzed Hydrocarbonylation of Alkenes. *Chem. Commun.* **1998**, No. 23, 2613–2614. https://doi.org/10.1039/a806722h.

(21) Drent, E.; Budzelaar, P. H. M. Palladium-Catalyzed Alternating Copolymerization of Alkenes and Carbon Monoxide. *Chem. Rev.* **1996**, *96* (2), 663–682. https://doi.org/10.1021/cr940282j.

(22) Kiss, G. Palladium-Catalyzed Reppe Carbonylation. *Chem. Rev.* **2001**, *101* (11), 3435–3456. https://doi.org/10.1021/cr010328q.

(23) Pospech, J.; Fleischer, I.; Franke, R.; Buchholz, S.; Beller, M. Alternative Metals for Homogeneous Catalyzed Hydroformylation Reactions. *Angew. Chem. Int. Ed.* **2013**, *52* (10), 2852–2872. https://doi.org/10.1002/anie.201208330.

(24) Sergeev, A. G.; Spannenberg, A.; Beller, M. Palladium-Catalyzed Formylation of Aryl Bromides: Elucidation of the Catalytic Cycle of an Industrially Applied Coupling Reaction. *J. Am. Chem. Soc.* **2008**, *130* (46), 15549–15563. https://doi.org/10.1021/ja804997z.

(25) Grushin, V. V. Hydrido Complexes of Palladium. *Chem. Rev.* **1996**, *96* (6), 2011–2034. https://doi.org/10.1021/cr950272y.

(26) Garrou, P. E.; Heck, R. F. The Mechanism of Carbonylation of Halo(Bis Ligand)Organoplatinum(II), -Palladium(II), and -Nickel(II) Complexes. *J. Am. Chem. Soc.* **1976**, *98* (14), 4115–4127. https://doi.org/10.1021/ja00430a018.

(27) Klingensmith, L. M.; Strieter, E. R.; Barder, T. E.; Buchwald, S. L. New Insights into Xantphos/Pd-Catalyzed C−N Bond Forming Reactions: A Structural and Kinetic Study. *Organometallics* **2006**, *25* (1), 82–91. https://doi.org/10.1021/om050715g.

(28) van Leeuwen, P. W. N. M.; Kamer, P. C. J.; Reek, J. N. H.; Dierkes, P. Ligand Bite Angle Effects in Metal-Catalyzed C−C Bond Formation. *Chem. Rev.* **2000**, *100* (8), 2741–2770. https://doi.org/10.1021/cr9902704.

(29) Martinelli, J. R.; Watson, D. A.; Freckmann, D. M. M.; Barder, T. E.; Buchwald, S. L. Palladium-Catalyzed Carbonylation Reactions of Aryl Bromides at Atmospheric Pressure: A General System Based on Xantphos. *J. Org. Chem.* **2008**, *73* (18), 7102–7107. https://doi.org/10.1021/jo801279r.

(30) Dahl, K.; Schou, M.; Amini, N.; Halldin, C. Palladium-Mediated [^{11}C]Carbonylation at Atmospheric Pressure: A General Method Using Xantphos as Supporting Ligand: Pd-Mediated [^{11} C]Carbonylation at Atmospheric Pressure. *Eur. J. Org. Chem.* **2013**, *2013* (7), 1228–1231. https://doi.org/10.1002/ejoc.201201708.

(31) For details, see the Supporting Information.

(32) Becica, J.; Dobereiner, G. E. Acceleration of Pd-Catalyzed Amide N-Arylations Using Cocatalytic Metal Triflates: Substrate Scope and Mechanistic Study. *ACS Catal.* **2017**, *7* (9), 5862–5870. https://doi.org/10.1021/acscatal.7b01317.

(33) Dekker, G. P. C. M.; Elsevier, C. J.; Vrieze, K.; van Leeuwen, P. W. N. M.; Roobeek, C. F. Influence of Ligands and Anions on the Insertion of Alkenes into Palladium-Acyl and Palladium-Carbomethoxy Bonds in the Neutral Complex (Dppp)Pd(C(O)CH_3)Cl and the Ionic Complexes [(P-P)PdR(L)]$^+SO_3CF_3^-$ (P-P = Dppe, Dppp, Dppb; R = C(O)CH_3, L = CH_3CN, PPh_3; R = C(O)OCH_3, L = PPh_3). *J. Organomet. Chem.* **1992**, *430* (3), 357–372. https://doi.org/10.1016/0022-328X(92)83271-I.

(34) Axet, M. R.; Castillon, S.; Claver, C. Rhodium-Diphosphite Catalysed Hydroformylation of Allylbenzene and Propenylbenzene Derivatives. *Inorganica Chim. Acta* **2006**, *359* (9), 2973–2979. https://doi.org/10.1016/j.ica.2005.12.039.

(35) Zhang, Z.; Wang, Q.; Chen, C.; Han, Z.; Dong, X.-Q.; Zhang, X. Selective Rhodium-Catalyzed Hydroformylation of Alkynes to α,β-Unsaturated Aldehydes with a Tetraphosphoramidite Ligand. *Org. Lett.* **2016**, *18* (13), 3290–3293. https://doi.org/10.1021/acs.orglett.6b01605.

(36) Fang, X.; Zhang, M.; Jackstell, R.; Beller, M. Selective Palladium-Catalyzed Hydroformylation of Alkynes to α,β-Unsaturated Aldehydes. *Angew. Chem. Int. Ed.* **2013**, *52* (17), 4645–4649. https://doi.org/10.1002/anie.201300759.

(37) Agabekov, V.; Seiche, W.; Breit, B. Rhodium-Catalyzed Hydroformylation of Alkynes Employing a Self-Assembling Ligand System. *Chem. Sci.* **2013**, *4* (6), 2418. https://doi.org/10.1039/c3sc50725d.

(38) Ishii, Y.; Miyashita, K.; Kamita, K.; Hidai, M. Selective Hydroformylation of Internal Acetylenes by $PdCl_2(PCy_3)_2$: Remarkable Synergistic Effect of Cobalt [1]. *J. Am. Chem. Soc.* **1997**, *119* (27), 6448–6449. https://doi.org/10.1021/ja9703887.

(39) Johnson, J. R.; Cuny, G. D.; Buchwald, S. L. Rhodium-Catalyzed Hydroformylation of Internal Alkynes Toα,β-Unsaturated Aldehydes. *Angew. Chem. Int. Ed. Engl.* **1995**, *34* (16), 1760–1761. https://doi.org/10.1002/anie.199517601.

(40) Tan, G.; Wu, Y.; Shi, Y.; You, J. Syngas-Free Highly Regioselective Rhodium-Catalyzed Transfer Hydroformylation of Alkynes to α,β-Unsaturated Aldehydes. *Angew. Chem. Int. Ed.* **2019**, *58* (22), 7440–7444. https://doi.org/10.1002/anie.201902553.

(41) Faria, J. V.; Vegi, P. F.; Miguita, A. G. C.; dos Santos, M. S.; Boechat, N.; Bernardino, A. M. R. Recently Reported Biological Activities of Pyrazole Compounds. *Bioorg. Med. Chem.* **2017**, *25* (21), 5891–5903. https://doi.org/10.1016/j.bmc.2017.09.035.

(42) Lan, R.; Liu, Q.; Fan, P.; Lin, S.; Fernando, S. R.; McCallion, D.; Pertwee, R.; Makriyannis, A. Structure−Activity Relationships of Pyrazole Derivatives as Cannabinoid Receptor Antagonists. *J. Med. Chem.* **1999**, *42* (4), 769–776. https://doi.org/10.1021/jm980363y.

(43) Seltzman, H. H. Recent CB1 Cannabinoid Receptor Antagonists and Inverse Agonists. *Drug Dev. Res.* **2009**, *70* (8), 601–615. https://doi.org/10.1002/ddr.20338.

(44) Böger, P.; Wakabayashi, K.; Hirai, K. *Herbicide Classes in Development: Mode of Action, Targets, Genetic Engineering, Chemistry*; Springer Berlin Heidelberg: Berlin, Heidelberg, 2002.

(45) Chinchilla, R.; Nájera, C. The Sonogashira Reaction: A Booming Methodology in Synthetic Organic Chemistry †. *Chem. Rev.* **2007**, *107* (3), 874–922. https://doi.org/10.1021/cr050992x.

(46) Zhang, X.; Kang, J.; Niu, P.; Wu, J.; Yu, W.; Chang, J. I_2 -Mediated Oxidative C–N Bond Formation for Metal-Free One-Pot Synthesis of Di-, Tri-, and Tetrasubstituted Pyrazoles from α,β-Unsaturated Aldehydes/Ketones and Hydrazines. *J. Org. Chem.* **2014**, *79* (21), 10170–10178. https://doi.org/10.1021/jo501844x.

(47) Lee, S. H.; Seo, H. J.; Lee, S.-H.; Jung, M. E.; Park, J.-H.; Park, H.-J.; Yoo, J.; Yun, H.; Na, J.; Kang, S. Y.; Song, K.-S.; Kim, M.; Chang, C.-H.; Kim, J.; Lee, J. Biarylpyrazolyl Oxadiazole as Potent, Selective, Orally Bioavailable Cannabinoid-1 Receptor Antagonists for the Treatment of Obesity. *J. Med. Chem.* **2008**, *51* (22), 7216–7233. https://doi.org/10.1021/jm800843r.

(48) Menozzi, G.; Schenone, P.; Mosti, L.; Mattioli, F. Synthesis of 5-Substituted 1-Aryl-1 *H* -Pyrazole-4-Acetonitriles, 4-Methyl-1-Phenyl-1 *H* -Pyrazole-3-Carbonitriles and Pharmacologically Active 1-Aryl-1 *H* -Pyrazole-4-Acetic Acids. *J. Heterocycl. Chem.* **1993**, *30* (4), 997–1002. https://doi.org/10.1002/jhet.5570300427.

(49) Genin, M. J.; Biles, C.; Keiser, B. J.; Poppe, S. M.; Swaney, S. M.; Tarpley, W. G.; Yagi, Y.; Romero, D. L. Novel 1,5-Diphenylpyrazole Nonnucleoside HIV-1 Reverse Transcriptase Inhibitors with Enhanced Activity versus the Delavirdine-Resistant P236L Mutant: Lead Identification and SAR of 3- and 4-Substituted Derivatives. *J. Med. Chem.* **2000**, *43* (5), 1034–1040. https://doi.org/10.1021/jm990383f.

(50) Portnoy, Moshe.; Frolow, Felix.; Milstein, David. Methanol Reduces an Organopalladium(II) Complex to a Palladium(I) Hydride. Crystallographic Characterization of a Hydrido-Bridged Palladium Complex. *Organometallics* **1991**, *10* (12), 3960–3962. https://doi.org/10.1021/om00058a007.

(51) Portnoy, M.; Milstein, D. A Binuclear Palladium(I) Hydride. Formation, Reactions, and Catalysis. *Organometallics* **1994**, *13* (2), 600–609. https://doi.org/10.1021/om00014a035.

(52) Toth, I.; Elsevier, C. J. Formation of Dinuclear Palladium(I) Hydride [Pd2(.Mu.-H)(.Mu.-CO){(S,S)-BDPP}2]Cl by Methanolysis or Hydrolysis of Pd(COMe)(Cl){(S,S)-BDPP} {(S,S)-BDPP = (2S,4S)-2,4-Bis(Diphenylphosphino)Pentane}. *Organometallics* **1994**, *13* (5), 2118–2122. https://doi.org/10.1021/om00017a084.

(53) Sperrle, M.; Gramlich, V.; Consiglio, G. Synthesis and Characterization of Cationic Palladium (6,6‘-Dimethoxybiphenyl-2,2‘-Diyl)Bis(Diphenylphosphine) Complexes. *Organometallics* **1996**, *15* (24), 5196–5201. https://doi.org/10.1021/om960445p.

(54) Siedle, A. R.; Newmark, R. A.; Gleason, W. B. Protonation of Phosphine Complexes of Zerovalent Nickel, Palladium, Platinum, and Ruthenium with Fluorocarbon Acids. *Inorg. Chem.* **1991**, *30* (9), 2005–2009. https://doi.org/10.1021/ic00009a012.

(55) Wang, J. Y.; Strom, A. E.; Hartwig, J. F. Mechanistic Studies of Palladium-Catalyzed Aminocarbonylation of Aryl Chlorides with Carbon Monoxide and Ammonia. *J. Am. Chem. Soc.* **2018**, *140* (25), 7979–7993. https://doi.org/10.1021/jacs.8b04073.

(56) Zuideveld, M. A.; Swennenhuis, B. H. G.; Boele, M. D. K.; Guari, Y.; van Strijdonck, G. P. F.; Reek, J. N. H.; Kamer, P. C. J.; Goubitz, K.; Fraanje, J.; Lutz, M.; Spek, A. L.; van Leeuwen, P. W. N. M. The Coordination Behaviour of Large

Natural Bite Angle Diphosphine Ligands towards Methyl and 4-Cyanophenylpalladium(Ii) Complexes. *J. Chem. Soc. Dalton Trans.* **2002**, No. 11, 2308. https://doi.org/10.1039/b111596k.

(57) Wiberg, K. B.; Crocker, L. S.; Morgan, K. M. Thermochemical Studies of Carbonyl Compounds. 5. Enthalpies of Reduction of Carbonyl Groups. *J. Am. Chem. Soc.* **1991**, *113* (9), 3447–3450. https://doi.org/10.1021/ja00009a033.

(58) Klähn, M.; Garland, M. V. On the Mechanism of the Catalytic Binuclear Elimination Reaction in Hydroformylation Systems. *ACS Catal.* **2015**, *5* (4), 2301–2316. https://doi.org/10.1021/cs5019925.

(59) Renny, J. S.; Tomasevich, L. L.; Tallmadge, E. H.; Collum, D. B. Method of Continuous Variations: Applications of Job Plots to the Study of Molecular Associations in Organometallic Chemistry. *Angew. Chem. Int. Ed.* **2013**, *52* (46), 11998–12013. https://doi.org/10.1002/anie.201304157.

(60) The reactions with the isolated intermediates occurred at slower rate than that with xantphos–PdI_2, most noticeable in case of reaction with **Pd_2-hydride**$^+$, most likely due to the lack of HI in the initial mixture of activated complexes (otherwise formed during the activation of xantphos–PdI_2, i.e., xantphos–PdI_2 + H_2 -> xantphos–PdHI + HI); HI oxidizes reduced Pd(I) species to active Pd(II) species – see Figure 8.

(61) Mardirossian, N.; Head-Gordon, M. Thirty Years of Density Functional Theory in Computational Chemistry: An Overview and Extensive Assessment of 200 Density Functionals. *Mol. Phys.* **2017**, *115* (19), 2315–2372. https://doi.org/10.1080/00268976.2017.1333644.

(62) Zhao, Y.; Truhlar, D. G. Density Functionals with Broad Applicability in Chemistry. *Acc. Chem. Res.* **2008**, *41* (2), 157–167. https://doi.org/10.1021/ar700111a.

(63) Subsequent binding of CO to xantphos–Pd-CO to furnish xantphos–$Pd(CO)_2$ has been calculated to be exergonic by –4.4 kcal/mol. This process can therefor still lower the energies of the mononuclear hydride species and subsequent binuclear transition states (Figure 6) relative to the mononuclear transition states (Figure 7).

(64) Carrow, B. P.; Hartwig, John. F. Ligandless, Anionic, Arylpalladium Halide Intermediates in the Heck Reaction. *J. Am. Chem. Soc.* **2010**, *132* (1), 79–81. https://doi.org/10.1021/ja909306f.

(65) Schroeter, F.; Soellner, J.; Strassner, T. Cross-Coupling Catalysis by an Anionic Palladium Complex. *ACS Catal.* **2017**, *7* (4), 3004–3009. https://doi.org/10.1021/acscatal.6b03655.

(66) Kolter, M.; Böck, K.; Karaghiosoff, K.; Koszinowski, K. Anionic Palladium(0) and Palladium(II) Ate Complexes. *Angew. Chem. Int. Ed.* **2017**, *56* (43), 13244–13248. https://doi.org/10.1002/anie.201707362.

(67) Johansson Seechurn, C. C. C.; Sperger, T.; Scrase, T. G.; Schoenebeck, F.; Colacot, T. J. Understanding the Unusual Reduction Mechanism of Pd(II) to Pd(I): Uncovering Hidden Species and Implications in Catalytic Cross-Coupling Reactions. *J. Am. Chem. Soc.* **2017**, *139* (14), 5194–5200. https://doi.org/10.1021/jacs.7b01110.

(68) Wagner, J. P.; Schreiner, P. R. London Dispersion in Molecular Chemistry-Reconsidering Steric Effects. *Angew. Chem. Int. Ed.* **2015**, *54* (42), 12274–12296. https://doi.org/10.1002/anie.201503476.

(69) Pollice, R.; Bot, M.; Kobylianskii, I. J.; Shenderovich, I.; Chen, P. Attenuation of London Dispersion in Dichloromethane Solutions. *J. Am. Chem. Soc.* **2017**, *139* (37), 13126–13140. https://doi.org/10.1021/jacs.7b06997.

(70) Yang, L.; Adam, C.; Nichol, G. S.; Cockroft, S. L. How Much Do van Der Waals Dispersion Forces Contribute to Molecular Recognition in Solution? *Nat. Chem.* **2013**, *5* (12), 1006–1010. https://doi.org/10.1038/nchem.1779.

(71) Broussard, M. E.; Juma, B.; Train, S. G.; Peng, W.-J.; Laneman, S. A.; Stanley, G. G. A Bimetallic Hydroformylation Catalyst: High Regioselectivity and Reactivity Through Homobimetallic Cooperativity. *Science* **1993**, *260* (5115), 1784–1788. https://doi.org/10.1126/science.260.5115.1784.

(72) Fernando, R. G.; Gasery, C. D.; Moulis, M. D.; Stanley, G. G. Bimetallic Homogeneous Hydroformylation. In *Homo- and Heterobimetallic Complexes in Catalysis*; Kalck, P., Ed.; Springer International Publishing: Cham, 2016; Vol. 59, pp 1–29. https://doi.org/10.1007/3418_2015_147.

(73) Liu, J.; Li, H.; Spannenberg, A.; Franke, R.; Jackstell, R.; Beller, M. Selective Palladium-Catalyzed Aminocarbonylation of Olefins to Branched Amides. *Angew. Chem. Int. Ed.* **2016**, *55* (43), 13544–13548. https://doi.org/10.1002/anie.201605104.

(74) Li, H.; Dong, K.; Jiao, H.; Neumann, H.; Jackstell, R.; Beller, M. The Scope and Mechanism of Palladium-Catalysed Markovnikov Alkoxycarbonylation of Alkenes. *Nat. Chem.* **2016**, *8* (12), 1159–1166. https://doi.org/10.1038/nchem.2586.